

# Effect of dark matter interaction on hybrid star in the light of the recent astrophysical observations

Suman Pal<sup></sup>, <sup>a,b,1</sup> Gargi Chaudhuri<sup></sup> <sup>a,b</sup>

<sup>a</sup>Physics Group, Variable Energy Cyclotron Centre, 1/AF Bidhan Nagar, Kolkata 700064, India

<sup>b</sup>Homi Bhabha National Institute, Training School Complex, Anushakti Nagar, Mumbai 400085, India

E-mail: [sumanvecc@gmail.com](mailto:sumanvecc@gmail.com), [gargi@vecc.gov.in](mailto:gargi@vecc.gov.in)

**Abstract.** We have explored the effect of dark matter interaction on hybrid star (HS) in the light of recent astrophysical observational constraints. The presence of dark matter is assumed to be there in both the hadron as well as the quark sector. The dark matter particle interacts with both hadron and quark matter through the exchange of a scalar as well as a vector meson. The equation of state (EOS) of the hadron part is computed using the NL3 version of the relativistic mean field(RMF) model, whereas the quark part is taken care of using the well-known MIT Bag model with the vector interaction. We investigate the effect of the dark matter density and the mass of the dark matter particle on various observables like mass, radius, tidal deformability of the dark matter admixed hybrid star(DMAHS). In this study, we have noted an intriguing aspect that is the speed of sound in the DMAHS is insensitive to both the mass as well as the density of dark matter. We also observe a striking similarity in the variation of transition mass and its corresponding radius, as well as the maximum mass of neutron stars, with dark matter density and mass. We employ observational constraints from neutron stars to narrow down the allowed range of the parameters of dark matter.

---

<sup>1</sup>Corresponding author

---

## Contents

<b>1</b>	<b>Introduction</b>	<b>1</b>
<b>2</b>	<b>Formalism</b>	<b>2</b>
2.1	Hadron Matter with admixed dark matter	3
2.2	Quark Matter admixed dark matter	4
2.3	Parameter configuration for the dark sector	7
<b>3</b>	<b>Results</b>	<b>8</b>
<b>4</b>	<b>Summary and conclusion</b>	<b>12</b>

---

## 1 Introduction

The study of neutron stars is highly interesting and challenging as it encompasses knowledge from different branches of physics, namely thermodynamics to statistical mechanics and also from general theory of relativity to particle and nuclear physics. The recent observational data on the highest as well as the lowest neutron star mass put severe constraints on the equation of state and composition of the neutron stars. Compact star equation of state is constrained by astrophysical observation such as maximum mass from PSRJ0740+6620 [1], NICER constraints on the radius of PSRJ0740+6620 and PSRJ0030+0451[2, 3]. The radius and mass measurement of *HESS*J1731 – 347[4] will be among the lightest and smallest compact objects ever detected. The gravitational wave observational[5–7] data limits the dimensionless tidal deformability of the  $1.4M_{\odot}$ .

Observational data from cosmology and astrophysics have predicted the presence of a new type of undiscovered matter, called dark matter which is expected to constitute a major part of the universe. The strongest and most straightforward evidence supporting the existence of dark matter on the scale of galaxies arises from observations of rotation curves. These curves depict the velocities at which stars and gas orbit around a galaxy's center relative to their distance from that center. Evidence also comes from the observation of the gravitational lensing and X-ray analysis of bullet clusters [8, 9]. The measurement of the cosmic microwave background anisotropy map indicates that dark matter likely makes up around 26% of the total matter in the universe, whereas only approximately 4% consists of baryonic matter. The study of dark matter is one of the most interesting and intriguing topics of theoretical cosmology. Presently, there exist several promising particle candidates for dark matter, including weakly interacting dark matter [10, 11] and axions, among others. Exploration of the detectability of these particles have unveiled a wide array of promising experimental setups, spanning from highly precise tabletop experiments to the integration of astronomical surveys and gravitational wave observations. One must visit these [12, 13] for a detailed review on the recent status of knowledge about this mysterious object called dark matter.

There has been increasing attention on indications of dark matter capture within compact stellar objects[10, 11, 14–20] and testing dark decays of baryons in Neutron Stars [21, 22]. Neutron stars are often referred to as "graveyards" for charged dark matter because they can potentially capture and accumulate this mysterious form of matter due to their immense

gravitational pull[14] The existence of dark matter inside neutron stars may be attributed to the capture or accretion of dark matter particles when the NS passes through the dark matter halo; conversion of neutrons to scalar dark matter or scalar DM production via bremsstrahlung are the other mechanisms which leads to increase in DM density inside NS. In Ref. [23] it has been pointed out that DM accumulation inside NS might be more for binary neutron star systems. The possibility of dark matter interacting with normal matter through gravitational interaction can affect the macroscopic properties of stellar objects like neutron stars. Due to their high compactness neutron star could trap the dark matter particles, which will rapidly thermalize and become accrued inside the neutron star. Since there is a lot of uncertainty in the knowledge of the properties of dark matter(DM), different models [24–28] have been considered where the nature of DM present in neutron stars can be fermionic or bosonic. At low temperatures relevant for the cold matter in NS, bosonic (spinless dark matter particles) DM exists in the form of Bose-Einstein Condensate (BEC). In this work, we will confine our study to fermionic dark matter only. Dark matter may be self-interacting and in such cases, the masses of the DM fermion and the DM mediators are constrained by the self-interaction constraints from bullet cluster.

The existence of DM admixed hadronic compact stars has been thoroughly discussed in the literature [25, 27] However relatively few works[29] throw light on the presence of dark matter in hybrid stars, that is the neutron stars with a quark core. In the present work, we consider hybrid stars with an admixture of dark matter. We have used the very commonly used Maxwell construction[30] to build the hybrid star where local charge neutrality has been obeyed by the quark and the hadronic phase. For the hadronic phase, the relativistic mean field (RMF) model[31] have been used while for the quark phase, the MIT Bag Model[30–32] modified by the vector interaction is considered. In the literature, the presence of dark matter inside the neutron stars is studied by considering the interaction of baryonic matter with dark matter by the exchange of Higgs Boson interaction [33–38] as well as the exchange of scalar and vector interaction [24, 39, 40]. In this work the interaction between dark matter and hadronic matter, as well as quark matter, will be considered though the exchange of one scalar and one vector meson. A distinct advantage of this model lies in the fact one can apply the single-fluid Tolman-Oppenheimer-Volkoff (TOV) equation where the DM is assumed to be uniformly distributed within NS. The other possibility is considering only gravitational interaction between dark matter(DM) and baryonic matter resulting in two fluid TOV equations [41] in place of the single fluid. In this scenario, one needs to specify the fraction of dark matter mass  $f_D$ [19]. Another aspect is that there is a wide mass range of the dark matter particle from  $10^{-12}$  eV to  $10^{15}$  GeV. In the context of the hybrid star, we are considering the values of  $m_\chi$  from 0.1 GeV to 100 GeV.

This paper is organized as follows. In Sec. 2 we give the detailed formalism of the equation of state both for hadronic and quark matter with admixed dark matter. In Sec.3 we show the numerical results. Finally, we summarize in Sec. 4

## 2 Formalism

The current study focuses on exploring the properties of hybrid stars within the context of dark matter admixture. We utilize the relativistic mean field model to describe the hadronic phase and the MIT bag model with vector interactions to describe the quark matter phase.

## 2.1 Hadron Matter with admixed dark matter

In this work, a uniformly distributed fermionic dark matter is considered to be present inside a neutron star. Dark matter( $\chi$ ) interacts via attractive scalar( $\phi$ ) and vector dark mesons( $\xi$ ). These meson fields also interact feebly with the nucleonic fields. We consider the relativistic mean field (RMF) model along with the dark matter[24, 29, 34, 39, 42]. As a result, the Lagrangian takes the form :

$$\begin{aligned} \mathcal{L}_{\text{HAD}} = & \bar{\psi}(i\gamma^\mu\partial_\mu - m_N)\psi + g_\sigma\bar{\psi}\psi - g_\omega\bar{\psi}\gamma^\mu\omega_\mu\psi - \frac{g_\rho}{2}\bar{\psi}\gamma^\mu\vec{\rho}_\mu\vec{\tau}\psi + \frac{1}{2}(\partial^\mu\sigma\partial_\mu\sigma - m_\sigma^2\sigma^2) \\ & - \frac{1}{4}\Omega^{\mu\nu}\Omega_{\mu\nu} + \frac{1}{2}m_\omega^2\omega_\mu\omega^\mu - \frac{1}{3}bm_N(g_\sigma\sigma)^3 - \frac{c}{4}(g_\sigma\sigma)^4 - \frac{1}{4}\vec{\rho}^{\mu\nu}\vec{\rho}_{\mu\nu} + \frac{1}{2}m_\rho^2\vec{\rho}_\mu\vec{\rho}^\mu, \quad (2.1) \end{aligned}$$

$$\begin{aligned} \mathcal{L}_{\text{total}} = & \bar{\chi}(i\gamma^\mu\partial_\mu - m_\chi)\chi + y_\phi\bar{\chi}\chi + y_\xi\bar{\chi}\gamma^\mu\xi_\mu\chi + g_\phi\bar{\chi}\psi + g_\xi\bar{\psi}\gamma^\mu\xi_\mu\psi \\ & + \frac{1}{2}m_\xi^2\xi_\mu\xi^\mu - \frac{1}{4}\xi_{\mu\nu}\xi^{\mu\nu} + \frac{1}{2}(\partial^\mu\phi\partial_\mu\phi - m_\phi^2\phi^2) + \mathcal{L}_{\text{HAD}} \end{aligned}$$

where  $\psi$  is the nucleonic field with mass  $m_N$ ,  $\chi$  is the dark matter field with mass  $m_\chi$ ;  $\sigma$ ,  $\omega^\mu$  and  $\vec{\rho}^\mu$  are the scalar, vector and isovector meson fields, respectively. Here  $\mathcal{L}_{\text{HAD}}$  is the pure hadronic part.  $\mathcal{L}_{\text{HAD}}$  contains five coupling constants :  $g_\sigma$ ,  $g_\omega$ ,  $g_\rho$ ,  $b$  and  $c$ . The coupling constants are determined by fixing the nuclear saturation properties. In this work, we are using NL3 parametrization with the following nuclear saturation parameters: nuclear saturation density ( $\rho_0$ ) =  $0.148\text{fm}^{-3}$ , binding energy per nucleon ( $\frac{BE}{A}$ ) =  $-16.24$  MeV, the incompressibility coefficient ( $K_{\text{sat}}$ ) =  $271.5$  MeV, effective mass ( $\frac{m^*}{m}$ ) =  $0.55$ , symmetry energy at saturation ( $E_{\text{sym}}$ ) =  $37.29$  MeV and the slope of the symmetry energy at saturation ( $L_{\text{sym}}$ ) =  $118.2$  MeV based on Ref [43–45]. The values of the hadronic parameters are given in the table 1. The parameters of the dark sector are given in the sub-section 2.3.

**Table 1:** The coupling constants of the NL3 model for the hadronic sector.

$m_\sigma$ (MeV)	$g_\sigma^2$	$m_\omega$ (MeV)	$g_\omega^2$	$m_\rho$ (MeV)	$g_\rho^2$	$b$	$c$
508.194	104.3871	782.5	165.5854	763	79.6	0.00205	-0.0026508

We use the relativistic mean field approximation, replacing the meson field with their mean fields. Our lagrangian includes a total of five meson fields, namely,  $\sigma$ ,  $\omega$ ,  $\rho$ ,  $\phi$  and  $\xi$ . The meson field equations are :

$$\begin{aligned} m_\sigma^2\sigma_0 &= g_\sigma \sum_{f=p,n} \rho_{sf} - bm(g_\sigma\sigma_0)^2 - cg_\sigma(g_\sigma\sigma_0)^3, \\ m_\omega^2\omega_0 &= g_\omega \sum_{f=p,n} \rho_f, \\ m_\rho^2\rho_{30} &= \frac{1}{2} \sum_{f=p,n} \tau_3\rho_f, \\ m_\phi^2\phi_0 &= g_\phi \sum_{f=p,n} \rho_{sf} + y_\phi\rho_{s\chi}, \\ m_\xi^2\xi_0 &= g_\xi \sum_{f=p,n} \rho_f + y_\xi\rho_\chi. \end{aligned} \quad (2.2)$$

Due to the interaction with scalar mesons the mass of the nucleons and dark matter particles are modified as

$$\begin{aligned} m_N^* &= m_N - g_\sigma \sigma_0 - g_\phi \phi_0 , \\ m_\chi^* &= m_\chi - y_\phi \phi_0 . \end{aligned} \quad (2.3)$$

The scalar and vector densities are expressed as follows:

$$\begin{aligned} \rho_{sf} &= \frac{m_N^*}{\pi^2} \int_0^{k_f} \frac{k^2}{\sqrt{(k^2 + (m_N^*)^2)}} dk , \\ \rho_{s\chi} &= \frac{m_\chi^*}{\pi^2} \int_0^{k_{f\chi}} \frac{k^2}{\sqrt{(k^2 + (m_\chi^*)^2)}} dk , \\ \rho_f &= \frac{k_f^3}{3\pi^2} , \\ \rho_\chi &= \frac{k_{f\chi}^3}{3\pi^2} . \end{aligned} \quad (2.4)$$

Here  $\rho_f$  is the baryon density for the proton and neutron and  $\rho_\chi$  is dark matter density corresponding to the fermi momentum  $k_{f\chi}$ . Due to the interaction of vector mesons, the chemical potential of the nucleon and dark matter particle gets modified as :

$$\begin{aligned} \mu_f &= \sqrt{k_f^2 + m_N^{*2}} + g_\omega \omega_0 + \tau_3 \frac{1}{2} g_\rho \rho_{30} + g_\xi \xi_0 , \\ \mu_\chi &= \sqrt{k_{f\chi}^2 + m_\chi^{*2}} + g_\xi \xi_0 . \end{aligned} \quad (2.5)$$

The energy and pressure are given by the following expressions as

$$\begin{aligned} \varepsilon &= \frac{1}{2} m_\sigma^2 \sigma_0^2 + \frac{1}{2} m_\omega^2 \omega_0^2 + \frac{1}{2} m_\rho^2 \rho_{30}^2 + \frac{1}{2} m_\phi^2 \phi_0^2 + \frac{1}{2} m_\xi^2 \xi_0^2 + \sum_{f=p,n} \int_0^{k_f} \frac{\gamma_f}{2\pi^2} \sqrt{k_f^2 + (m_N^*)^2} k^2 dk + \\ &\quad \int_0^{k_{f\chi}} \frac{\gamma_f}{2\pi^2} \sqrt{k_f^2 + (m_\chi^*)^2} k^2 dk + \frac{1}{3} b m_N (g_\sigma \sigma)^3 + \frac{c}{4} (g_\sigma \sigma)^4 , \\ P &= -\frac{1}{2} m_\sigma^2 \sigma_0^2 + \frac{1}{2} m_\omega^2 \omega_0^2 + \frac{1}{2} m_\rho^2 \rho_{30}^2 - \frac{1}{2} m_\phi^2 \phi_0^2 + \frac{1}{2} m_\xi^2 \xi_0^2 + \sum_{f=p,n} \int_0^{k_f} \frac{\gamma_f}{6\pi^2} \frac{k^4}{\sqrt{k_f^2 + (m_N^*)^2}} dk + \\ &\quad \int_0^{k_{f\chi}} \frac{\gamma_f}{6\pi^2} \frac{k^4}{\sqrt{k_f^2 + (m_\chi^*)^2}} dk - \frac{1}{3} b m_N (g_\sigma \sigma)^3 - \frac{c}{4} (g_\sigma \sigma)^4 . \end{aligned} \quad (2.6)$$

## 2.2 Quark Matter admixed dark matter

We utilize the MIT bag model with vector interaction to characterize the combination of quark matter and dark matter. We explore feeble interaction between fermionic dark matter and strange quark matter within a quark star, mediated by scalar and vector dark bosons.

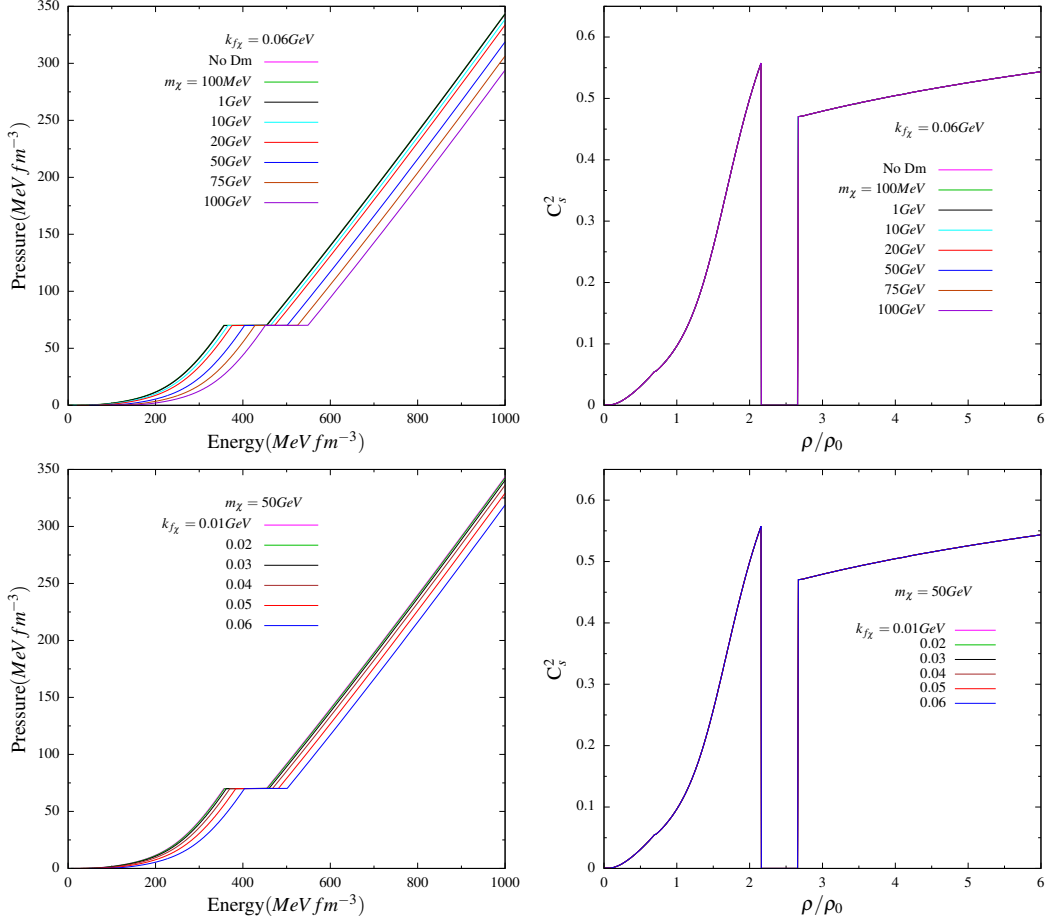


**Figure 1:** Pressure vs energy density (left panel) and speed of sound vs baryon density (right panel) for a dark matter admixed hybrid star; different values of  $m_\chi$  with fixed  $k_{f_\chi} = 0.06$  GeV (upper panel) and different values of  $k_{f_\chi}$  with fixed  $m_\chi = 50$  GeV (lower panel)

As a result, the Lagrangian takes the form [24, 39, 40]:

$$\begin{aligned}
\mathcal{L} = & \sum_{f=u,d,s} [\bar{\psi}_f (i\gamma_\mu \partial^\mu - m_f) \psi_f - B] \Theta(\bar{\psi}_f \psi_f) - \sum_{f=u,d,s} [\bar{\psi}_f \gamma_\mu (g_V V^\mu - g_\xi \xi^\mu) \psi_f] \Theta(\bar{\psi}_f \psi_f) \\
& + \frac{1}{2} m_V^2 V_\mu V^\mu - \frac{1}{4} V_{\mu\nu} V^{\mu\nu} + \bar{\psi}_e (i\gamma_\mu \partial^\mu - m_e) \psi_e + \bar{\chi} (i\gamma_\mu \partial^\mu - y_\xi \gamma_\mu \xi^\mu - (m_\chi - y_\phi \phi)) \chi \\
& + \frac{1}{2} m_\xi^2 \xi_\mu \xi^\mu - \frac{1}{4} \xi_{\mu\nu} \xi^{\mu\nu} + \frac{1}{2} (\partial^\mu \phi \partial_\mu \phi - m_\phi^2 \phi^2)
\end{aligned} \tag{2.7}$$

Here quark interaction is mediated by one attractive scalar dark meson ( $\phi$ ) and two vectors (V (normal) and  $\xi$  (dark)) repulsive mesons. The bag constant (B) is added to the Lagrangian to reflect the quark confinement. The normal vector interaction coupling constant ( $g_V$ ) is scaled with  $G_V = \left(\frac{g_V}{m_V}\right)^2$ , where  $m_V$  is the mass of the vector meson (V). The interaction between the quark sector and dark boson is taken to be feeble as mentioned in [40]. In this work, we consider the masses of the quarks to be  $m_u = 2.16$  MeV,  $m_d = 4.67$  MeV and  $m_s = 93.4$  MeV and vector coupling constant  $G_V = 0.35$   $\text{fm}^{-2}$ . After the mean-field

approximation, the equation of motion of the meson fields are given as

$$\begin{aligned}
m_V^2 V_0 &= g_V \sum_{f=u,d,s} \rho_f , \\
m_\xi^2 \xi_0 &= g_\xi \sum_{f=u,d,s} \rho_f + y_\xi \rho_\chi , \\
m_\phi^2 \phi_0 &= g_\phi \sum_{f=u,d,s} \rho_{sf} + y_\phi \rho_{s\chi} .
\end{aligned} \tag{2.8}$$

The expressions for the scalar and vector densities for the quark admixed dark matter configuration are as follows:

$$\begin{aligned}
\rho_{sf} &= \frac{m_f^*}{\pi^2} \int_0^{k_f} \frac{k^2}{\sqrt{(k^2 + (m_f^*)^2)}} dk , \\
\rho_{s\chi} &= \frac{m_\chi^*}{\pi^2} \int_0^{k_{f\chi}} \frac{k^2}{\sqrt{(k^2 + (m_\chi^*)^2)}} dk , \\
\rho_f &= \frac{k_f^3}{\pi^2} , \\
\rho_\chi &= \frac{k_{f\chi}^3}{3\pi^2} .
\end{aligned} \tag{2.9}$$

In the MIT bag model, the quark mass is conventionally treated as constant. However, when incorporating the scalar boson ( $\phi$ ), both the quark mass and the mass of dark matter undergo modifications.

$$\begin{aligned}
m_f^* &= m_f - g_\phi \phi_0 , \\
m_\chi^* &= m_\chi - y_\phi \phi_0 .
\end{aligned} \tag{2.10}$$

Because of the vector interaction, there are modifications to the chemical potentials of both quarks and dark matter.

$$\begin{aligned}
\mu_f &= \sqrt{k_f^2 + (m_f^*)^2} + g_V V_0 + g_\xi \xi_0 , \\
\mu_\chi &= \sqrt{k_{f\chi}^2 + (m_\chi^*)^2} + y_\xi \xi_0 .
\end{aligned} \tag{2.11}$$

The energy and pressure expressions are given by

$$\begin{aligned}
\varepsilon &= \frac{1}{2} m_V^2 V_0^2 + \frac{1}{2} m_\xi^2 \xi_0^2 + \frac{1}{2} m_\phi^2 \phi_0^2 + B + \frac{\gamma_f}{2\pi^2} \sum_{f=u,d,s} \int_0^{k_f} \sqrt{k^2 + (m_f^*)^2} k^2 dk \\
&\quad + \frac{\gamma_e}{2\pi^2} \int_0^{k_e} \sqrt{k^2 + m_e^2} k^2 dk + \frac{\gamma_\chi}{2\pi^2} \int_0^{k_{f\chi}} \sqrt{k^2 + (m_\chi^*)^2} k^2 dk , \\
P &= \frac{1}{2} m_V^2 V_0^2 + \frac{1}{2} m_\xi^2 \xi_0^2 - \frac{1}{2} m_\phi^2 \phi_0^2 - B + \frac{\gamma_f}{6\pi^2} \sum_{f=u,d,s} \int_0^{k_f} \frac{k^4}{\sqrt{k^2 + (m_f^*)^2}} dk \\
&\quad + \frac{\gamma_e}{6\pi^2} \int_0^{k_e} \frac{k^4}{\sqrt{k^2 + m_e^2}} dk + \frac{\gamma_\chi}{6\pi^2} \int_0^{k_{f\chi}} \frac{k^4}{\sqrt{k^2 + (m_\chi^*)^2}} dk .
\end{aligned} \tag{2.12}$$

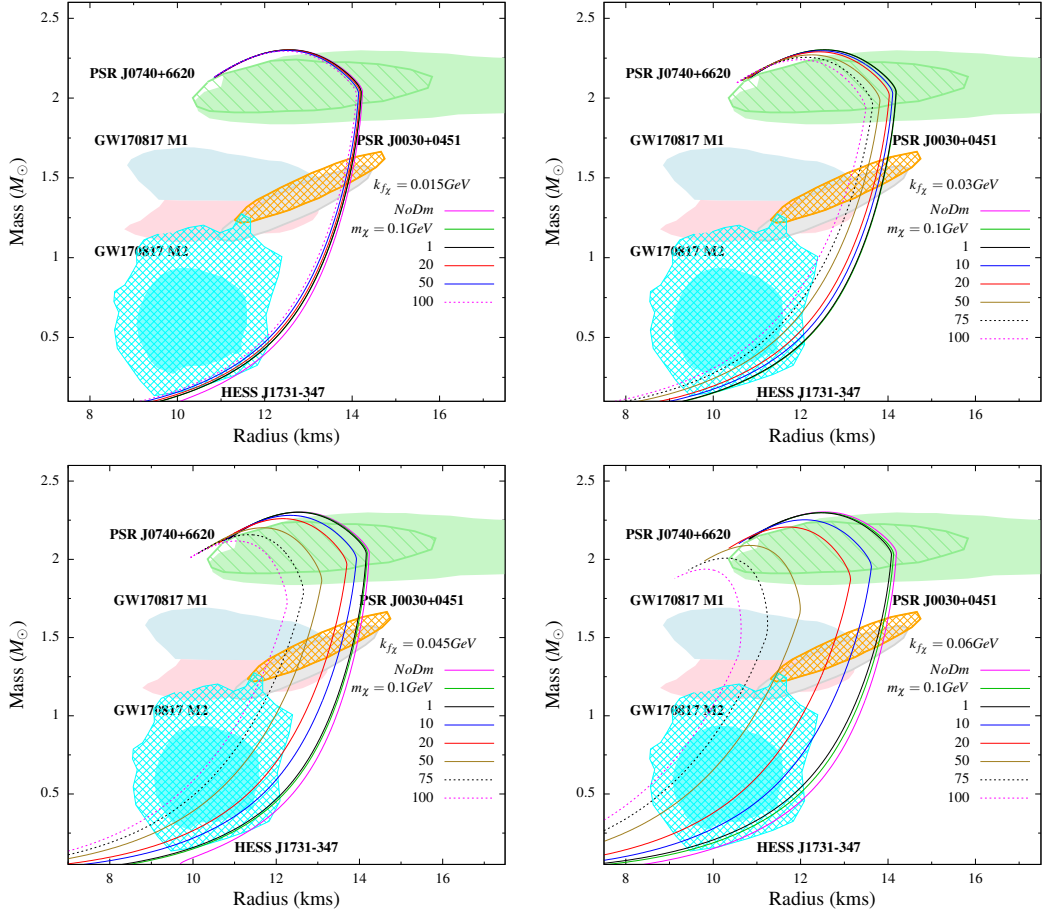


**Figure 2:** Mass-radius diagram corresponding to the different values of  $m_\chi$  with fixed  $k_{f_\chi} = 0.015, 0.03, 0.045$  and  $0.06$  GeV. The restrictions on the M-R plane from GW170817, the NICER experiment for PSR J0030+0451 PSR J0740+6620, and HESSJ1731-347 have been incorporated.

### 2.3 Parameter configuration for the dark sector

In this work, we assume that the average dark matter number density inside the neutron star is  $10^3$  times smaller than the saturated nuclear matter density, and we assume that the Fermi momentum of the dark matter remains constant throughout the neutron star. In our calculations, we explore a range of dark matter Fermi momenta, with values ranging from approximately 0.01 to 0.06 GeV.

We consider the dark matter self-interaction constraints from the bullet cluster, for the DM fermions of mass  $\frac{\sigma_T}{m_\chi} = (0.1 - 10) \text{ cm}^2 \text{ g}^{-1}$  [9] Assuming the cross-section of the self-interaction to be

$$\sigma_\chi \sim 5 \times 10^{-23} \left( \frac{\alpha_x}{0.01} \right)^2 \left( \frac{m_\chi}{10 \text{ GeV}} \right)^2 \left( \frac{10 \text{ MeV}}{m_x} \right)^2 \text{ cm}^2 \quad (2.13)$$

where  $\alpha_x = \frac{g_x^2}{4\pi}$  and  $G_x = \left( \frac{y_x}{m_x} \right)^2$  where x may be the scalar and vector mediator. We



have taken  $m_x = 10$  MeV , then

$$\frac{\sigma_\chi}{m_\chi} = 1.2 \times 10^{-4} \left( \frac{G_x}{1 \text{ fm}^2} \right) \left( \frac{m_\chi}{1 \text{ GeV}} \right) \text{ cm}^2/\text{gm} \quad (2.14)$$

For the lower bound, we take  $\frac{\sigma_\chi}{m_\chi} = 0.1 \text{ cm}^2\text{gm}^{-1}$ , which gives rise to  $y_x = 0.2687 \left( \frac{1 \text{ GeV}}{m_\chi} \right)^{\frac{1}{4}}$ .

For the upper bound,  $\frac{\sigma_\chi}{m_\chi} = 10 \text{ cm}^2\text{gm}^{-1}$  gives rise to  $y_x = 1.511 \left( \frac{1 \text{ GeV}}{m_\chi} \right)^{\frac{1}{4}}$ .

The final limit on the dark matter to the dark scalar and vector boson couplings reads as

$$0.2687 \left( \frac{1 \text{ GeV}}{m_\chi} \right)^{\frac{1}{4}} \leq y_x \leq 1.511 \left( \frac{1 \text{ GeV}}{m_\chi} \right)^{\frac{1}{4}} \quad (2.15)$$

In this study, we have adopted the values of  $g_\xi$  and  $g_\phi$  to be approximately  $10^{-4}$ , as previously mentioned in reference [24, 40]. The values of  $m_\chi$  and  $y_x$  are given in table 2. For the nuclear sector, we have employed the NL3 parametrization, while for the quark sector, we have employed the vector bag model with a bag constant of  $B^{1/4} = 160$  MeV.

**Table 2:** The coupling constants of the dark sector.

$m_\chi$ (GeV)	$y_x$
0.1	2.2
1.0	1.0
10	0.8
20	0.7
50	0.4
100	0.1

### 3 Results

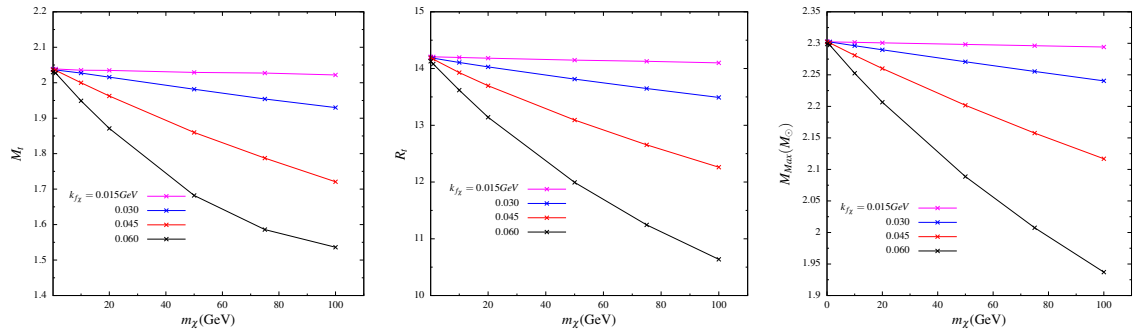


**Figure 3:** The variation of  $M_t$ (left),  $R_t$ (middle) and  $M_{Max}$ (right) with  $k_{f_\chi}$  for the different values of  $m_\chi$ .

In this work, the phase transition from hadronic to quark phase is obtained with Maxwell construction where the pressure and baryon chemical potential of the individual charge-neutral phases are equal. In Fig. 1 ( upper left panel) we plot the equation of state (EOS) for

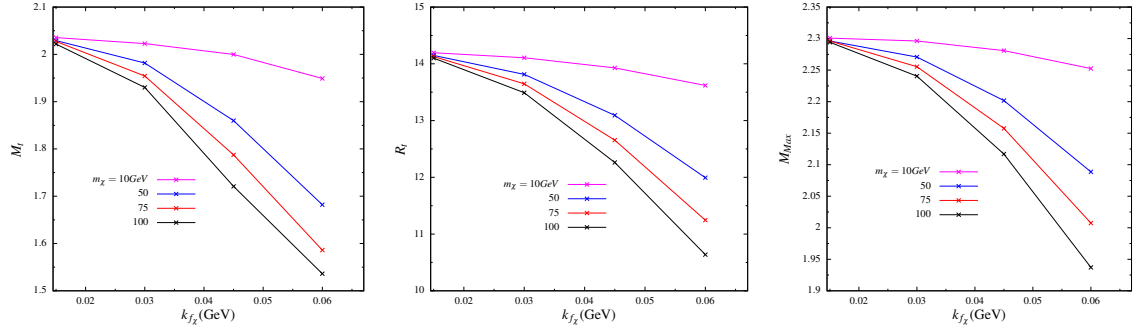


**Figure 4:** The variation of  $M_t$ (left),  $R_t$ (middle) and  $M_{Max}$ (right) with  $m_\chi$  for the different values of  $k_{f_\chi}$ .

different values of the mass of the DM particle ( $m_\chi$ ) for a fixed value of the dark matter Fermi momentum  $k_{f_\chi}$  ( $=0.06$  GeV). The results are pretty close to each other for the range of the masses used. In the upper right panel, we have plotted the square of the velocity of sound  $C_s^2$  for dark matter and it has been observed that this observable is insensitive to  $m_\chi$  and hence  $C_s^2$  remains unchanged irrespective of the values chosen. In the lower panel, we plot the EOS for different  $k_{f_\chi}$  keeping the mass of DM particle  $m_\chi$  fixed. Here also the plots are pretty close to each other for different values. In the right lower panel, we plot the corresponding  $C_s^2$ . It is once again observed that this is insensitive to DM parameters and cannot discriminate among the different values. From this figure, it seems that the effect of the dark matter is negligible, but this is not true. The reason being that the contribution from the dark matter kinetic energy term is much greater than the kinetic pressure integral. The kinetic energy and pressure integral do not vary much with baryon density. Therefore change in the pressure energy slope is negligible and it does not affect the speed of sound.

In Fig. 2, we plot the mass-radius of the hybrid stars for scaled coupling ( $G_V = 0.35 fm^{-2}$ ) for different values of the dark matter Fermi momentum  $k_{f_\chi}$ . For fixed  $k_{f_\chi}$ , in each figure we have shown the effect of the mass of the dark matter particle  $m_\chi$  on the mass and radius of the HS. In each figure, we have also indicated the plot for no dark matter case in order to clearly demonstrate the difference. When the dark matter fermi momentum ( $k_{f_\chi}$ ) (upper left figure) is low, there is not much difference between the plots as we vary the mass of the dark matter particle. This case of  $k_{f_\chi} = 0.015$  GeV satisfies the observational constraints from PSR J0030+0451 and PSR J0740+6620 but fails to satisfy those from Gravitational Wave observation and HESS J1731-347. As we increase the value of  $k_{f_\chi}$ , the effect of the mass of the dark matter particle  $m_\chi$  becomes more and more evident as seen in the other plots of Fig. 2. With the increase in the mass of the dark matter particle, the transition mass ( $M_t$ ) (where hadron to quark phase transition takes place), the maximum mass ( $M_{max}$ ) as well as the radius  $R_t$  (radius corresponding to  $M_t$ ) of the HS decreases. The results for higher mass DM particles satisfy the constraints from GW170817 as well as that from HESS J1731-347. Thus the understanding of the nature of the lightest observed neutron star *HESS J1731 – 347*, can be addressed from the possible scenario of the dark matter admixed hybrid star configuration. From Fig. 2. we see that massive dark matter and high Fermi momentum dark matter particles are more favorable to satisfy the *HESS J1731 – 347* constraints. It is also noticed that  $M_t$ ,  $M_{max}$ , as well as  $R_t$  of the HS decreases with  $k_{f_\chi}$ . These features will be further demonstrated in the next figures. In Fig. 3, we show the variation of  $M_t$ ,  $R_t$  and  $M_{max}$  with  $m_\chi$  for different values of  $k_{f_\chi}$ . When  $k_{f_\chi}$  is very small (0.015 GeV), there is almost negligible or no change of

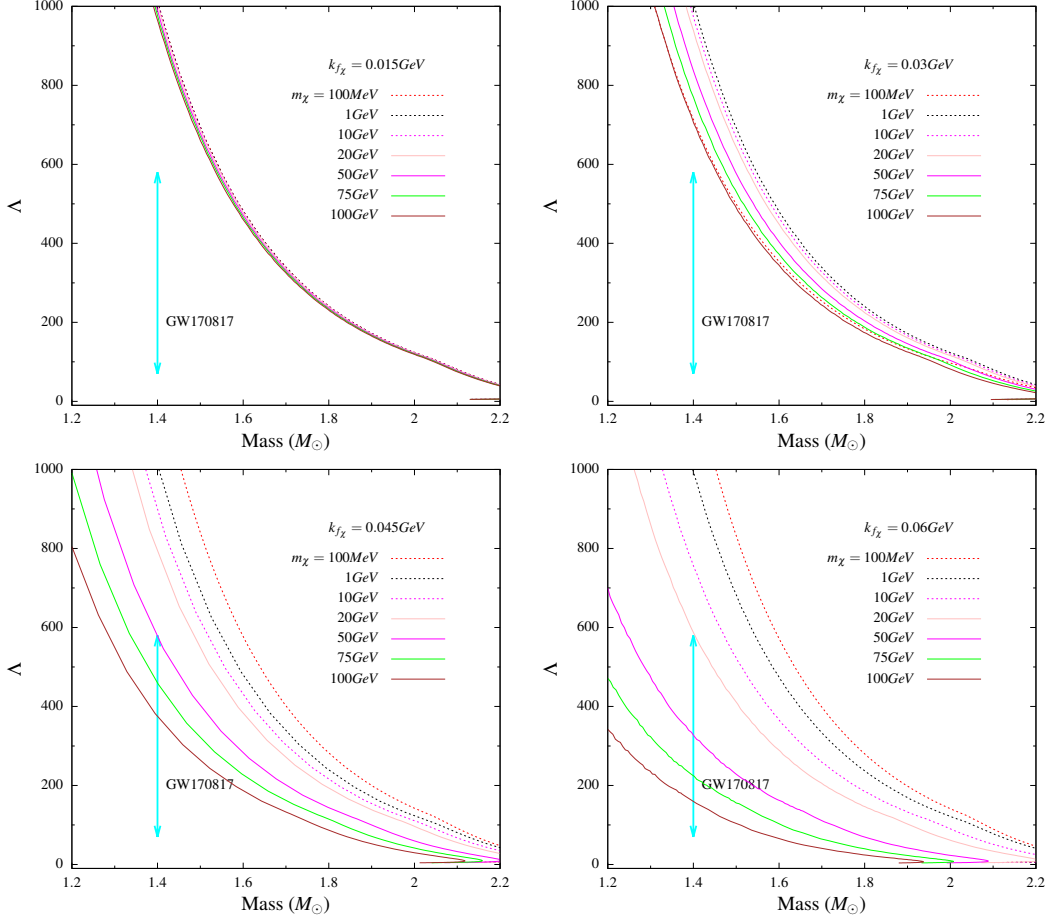


**Figure 5:** Tidal deformability-Mass diagram with different values of  $m_\chi$  with fixed  $k_{f_\chi} = 0.015$  (upper left), 0.03 (upper right), 0.045 (lower left) and 0.06 (lower right) GeV. The restrictions on the  $M - \lambda$  plane from GW170817 have been incorporated.

these parameters with mass of the DM particle. The decrease of these parameters becomes more noticeable as we increase the value of  $k_{f_\chi}$  and the change is most for the highest value (0.06 GeV) of  $k_{f_\chi}$ . For a fixed value of  $k_{f_\chi}$ , it is seen that the nature of variation of all the three parameters,  $M_t$ ,  $M_{max}$ , as well as  $R_t$ , is very similar as seen from Fig. 3. The fitted functional relationship of each of  $M_t$ ,  $R_t$  and  $M_{Max}$  with  $m_\chi$  is quite similar for a fixed value of dark matter fermi momentum. We demonstrate here only one such fitted functional form for the value of  $k_{f_\chi} = 0.06$  GeV as given below

$$\begin{aligned}
 M_t &= 2.3772 \times 10^{-5} (m_\chi^2 + m_\chi) + 2.03457 \exp\left(-\frac{m_\chi}{221.599}\right) \\
 R_t &= 8.1067 \times 10^{-5} (m_\chi^2 + m_\chi) + 14.1205 \exp\left(-\frac{m_\chi}{276.16}\right) \\
 M_{Max} &= 7.4639 \times 10^{-6} (m_\chi^2 + m_\chi) + 2.3004 \exp\left(-\frac{m_\chi}{473.882}\right)
 \end{aligned} \tag{3.1}$$

In Fig. 4 we plot  $M_t$ ,  $R_t$  and  $M_{max}$  as a function of  $k_{f_\chi}$  for fixed values of the DM particle mass  $m_\chi$ . It is observed that all the three parameters follow same pattern of variation with  $k_{f_\chi}$  irrespective of the dark matter particle mass  $m_\chi$ . The fitted relationship of  $M_t$ ,  $R_t$ ,  $M_{Max}$

with  $k_{f_\chi}$  are given below for  $m_\chi = 100 \text{ GeV}$

$$\begin{aligned} M_t &= 6281.98 k_{f_\chi}^3 - 809.756 k_{f_\chi}^2 + 19.9982 k_{f_\chi} + 1.88916 \\ R_t &= 10172.8 k_{f_\chi}^3 - 2246.67 k_{f_\chi}^2 + 42.3444 k_{f_\chi} + 13.985 \\ M_{Max} &= 567.407 k_{f_\chi}^3 - 203.533 k_{f_\chi}^2 + 4.618 k_{f_\chi} + 2.26992 \end{aligned} \quad (3.2)$$

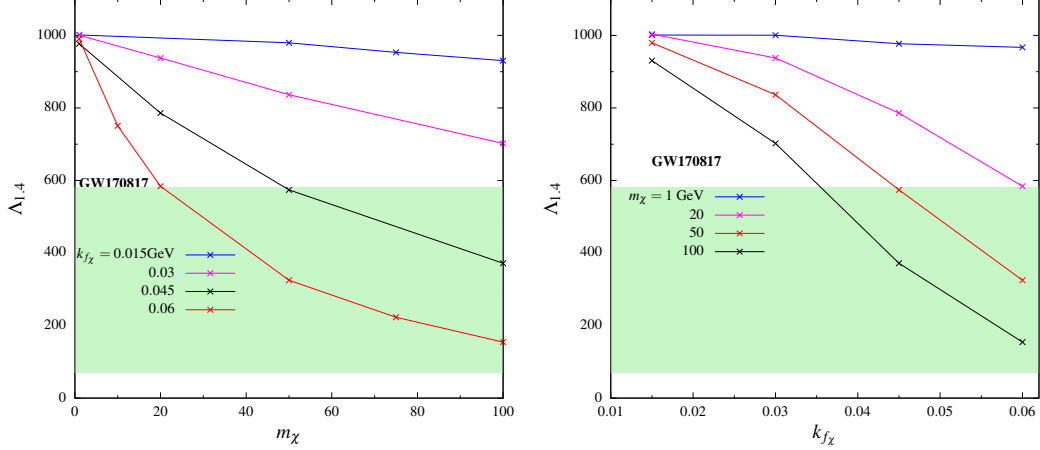


**Figure 6:** The variation of  $\Lambda_{1.4}$  with  $m_\chi$  for different values of  $k_{f_\chi}$  (left panel) and  $k_\chi$  for different values of  $m_\chi$  (right panel).

It is observed that all these variations follow the same parametrization with the coefficients of the expansion being different for different values of  $m_\chi$ . This is indeed a remarkable observation of the effect of the dark matter interaction on HS properties.

In Fig. 5, we show the variation of tidal deformability with mass. In each subfigure, we demonstrate the variation of tidal deformability with the mass of the dark matter particle keeping the fermi momentum  $k_{f_\chi}$  fixed. For low  $k_{f_\chi}$  (upper left figure), it is observed that tidal deformability is not sensitive to the mass of the dark matter particle  $m_\chi$  and also the constraints from GW170817 is not satisfied. As one increases the value of the Fermi momentum (upper right figure),  $\Lambda$  could better discriminate between the masses of the dark matter particle and those with higher masses do satisfy the constraints from the gravitational wave (GW) observation. From the lower panel, a similar trend continues to be observed with further increase in the value of  $k_{f_\chi}$ . The sensitivity of the tidal deformability parameter on the mass of the dark matter particle increases reaching its maximum for the maximum value of  $k_{f_\chi}$  used which is equal to 0.06 GeV. The range of  $m_\chi$  values satisfying the constraint from GW170817 increases with  $k_{f_\chi}$ . Masses of dark matter particle  $m_\chi$  spanning the range of 20 to 100 GeV obey the constraint for  $k_{f_\chi} = 0.06$  GeV. A similar trend has also been observed from the mass-radius plots in Fig. 2. We next study the effect  $m_\chi$  and  $k_{f_\chi}$  on  $\Lambda_{1.4}$  as shown in the Fig. 6. The value of  $\Lambda_{1.4}$  decreases with  $m_\chi$  and  $k_\chi$ . From the left panel of Fig. 6,  $\Lambda_{1.4}$  calculations reveal that the DM fermi momenta values  $k_{f_\chi} = 0.015$  GeV and  $k_{f_\chi} = 0.03$  GeV are restricted by GW170817 observation. The lower values of  $m_\chi$  are also restricted. In the right panel of the Fig. 6 it is inferred that DM particle mass up to  $m_\chi = 20$  GeV and fermi momenta up to  $k_{f_\chi} = 0.03$  GeV are not allowed by the  $\Lambda_{1.4}$  observation. We also observe that from the GW170817 tidal deformability constraint, the lower values of  $k_{f_\chi}$  and  $m_\chi$  are ruled out.

## 4 Summary and conclusion

In this work, we have investigated the dark matter accreted hybrid stars resulting in the formation of DM admixed hybrid stars. We use the RMF model with  $NL3$  parametrization for the hadronic sector and the MIT bag model with vector interactions for the quark sector; phase transition being achieved by using Maxwell construction. We have studied the effect of the dark matter parameters  $m_\chi$  and  $k_{f_\chi}$  on the equation of state, speed of sound, mass-radius relations, and tidal deformability of the HS. The important finding of our result is that the speed of sound is insensitive to the dark matter parameters ( $m_\chi$  and  $k_{f_\chi}$ ). In the  $M - R$  diagram, we find that PSRJ0740+6620 data is satisfied by most of our chosen parameters of DM except for the more massive and large momentum cases. PSRJ0030+0451 is satisfied by the all parameter set of our chosen model. We have constrained the mass and momentum range of the DM particle from the GW170817 constraint. We have also explored to find the possible nature of HESSJ1731-347 in the light of our dark matter admixed hybrid star model. In order to understand the effect of the dark matter parameters, we plot  $M_t, R_t$ , and  $M_{Max}$  with  $m_\chi$  and  $k_{f_\chi}$ . We find that all the above-mentioned parameters scale with the mass of the dark matter particle  $m_\chi$  in the same pattern for a given  $k_{f_\chi}$  and follow an universal parametrization. We also examine the dimensionless tidal deformability of  $1.4M_\odot$ . This investigation leads to narrowing down the admissible range of dark matter fermi momentum and mass.

## References

- [1] E. Fonseca et al., *Refined Mass and Geometric Measurements of the High-mass PSR J0740+6620*, *Astrophys. J. Lett.* **915** (2021) L12 [[2104.00880](#)].
- [2] T.E. Riley et al., *A NICER View of PSR J0030+0451: Millisecond Pulsar Parameter Estimation*, *Astrophys. J. Lett.* **887** (2019) L21 [[1912.05702](#)].
- [3] M.C. Miller et al., *PSR J0030+0451 Mass and Radius from NICER Data and Implications for the Properties of Neutron Star Matter*, *Astrophys. J. Lett.* **887** (2019) L24 [[1912.05705](#)].
- [4] V. Doroshenko, V. Suleimanov, G. Pühlhofer and A. Santangelo, *A strangely light neutron star within a supernova remnant*, *Nature Astronomy* **6** (2022) 1444.
- [5] LIGO SCIENTIFIC, VIRGO collaboration, *GW170817: Observation of Gravitational Waves from a Binary Neutron Star Inspiral*, *Phys. Rev. Lett.* **119** (2017) 161101 [[1710.05832](#)].
- [6] LIGO SCIENTIFIC, VIRGO collaboration, *GW190814: Gravitational Waves from the Coalescence of a 23 Solar Mass Black Hole with a 2.6 Solar Mass Compact Object*, *Astrophys. J. Lett.* **896** (2020) L44 [[2006.12611](#)].
- [7] LIGO SCIENTIFIC, VIRGO collaboration, *GW170817: Measurements of neutron star radii and equation of state*, *Phys. Rev. Lett.* **121** (2018) 161101 [[1805.11581](#)].
- [8] S.W. Randall, M. Markevitch, D. Clowe, A.H. Gonzalez and M. Bradac, *Constraints on the Self-Interaction Cross-Section of Dark Matter from Numerical Simulations of the Merging Galaxy Cluster 1E 0657-56*, *Astrophys. J.* **679** (2008) 1173 [[0704.0261](#)].
- [9] S. Tulin, H.-B. Yu and K.M. Zurek, *Beyond collisionless dark matter: Particle physics dynamics for dark matter halo structure*, *Phys. Rev. D* **87** (2013) 115007.
- [10] I. Goldman and S. Nussinov, *Weakly Interacting Massive Particles and Neutron Stars*, *Phys. Rev. D* **40** (1989) 3221.
- [11] C. Kouvaris, *WIMP Annihilation and Cooling of Neutron Stars*, *Phys. Rev. D* **77** (2008) 023006 [[0708.2362](#)].

- [12] G. Bertone, D. Hooper and J. Silk, *Particle dark matter: Evidence, candidates and constraints*, *Phys. Rept.* **405** (2005) 279 [[hep-ph/0404175](#)].
- [13] J. Bramante and N. Raj, *Dark matter in compact stars*, *Phys. Rept.* **1052** (2024) 1 [[2307.14435](#)].
- [14] A. Gould, B.T. Draine, R.W. Romani and S. Nussinov, *Neutron stars: Graveyard of charged dark matter*, *Physics Letters B* **238** (1990) 337.
- [15] M. Baryakhtar, J. Bramante, S.W. Li, T. Linden and N. Raj, *Dark Kinetic Heating of Neutron Stars and An Infrared Window On WIMPs, SIMPs, and Pure Higgsinos*, *Phys. Rev. Lett.* **119** (2017) 131801 [[1704.01577](#)].
- [16] N. Raj, P. Tanedo and H.-B. Yu, *Neutron stars at the dark matter direct detection frontier*, *Phys. Rev. D* **97** (2018) 043006 [[1707.09442](#)].
- [17] A. Joglekar, N. Raj, P. Tanedo and H.-B. Yu, *Dark kinetic heating of neutron stars from contact interactions with relativistic targets*, *Phys. Rev. D* **102** (2020) 123002 [[2004.09539](#)].
- [18] J. Bramante, B.J. Kavanagh and N. Raj, *Scattering Searches for Dark Matter in Subhalos: Neutron Stars, Cosmic Rays, and Old Rocks*, *Phys. Rev. Lett.* **128** (2022) 231801 [[2109.04582](#)].
- [19] W. Husain and A.W. Thomas, *Novel neutron decay mode inside neutron stars*, *J. Phys. G* **50** (2023) 015202 [[2206.11262](#)].
- [20] M. Deliyergiyev, A. Del Popolo and M.L. Delliou, *Neutron star mass in dark matter clumps*, *Mon. Not. Roy. Astron. Soc.* **527** (2023) 4483 [[2311.00113](#)].
- [21] D. McKeen, M. Pospelov and N. Raj, *Cosmological and astrophysical probes of dark baryons*, *Phys. Rev. D* **103** (2021) 115002 [[2012.09865](#)].
- [22] D. McKeen, M. Pospelov and N. Raj, *Neutron Star Internal Heating Constraints on Mirror Matter*, *Phys. Rev. Lett.* **127** (2021) 061805 [[2105.09951](#)].
- [23] L. Brayeur and P. Tinyakov, *Enhancement of dark matter capture by neutron stars in binary systems*, *Phys. Rev. Lett.* **109** (2012) 061301.
- [24] D. Sen and A. Guha, *Implications of feebly interacting dark sector on neutron star properties and constraints from GW170817*, *Mon. Not. Roy. Astron. Soc.* **504** (2021) 3354 [[2104.06141](#)].
- [25] B. Kain, *Dark matter admixed neutron stars*, *Phys. Rev. D* **103** (2021) 043009 [[2102.08257](#)].
- [26] D.R. Karkevandi, S. Shakeri, V. Sagun and O. Ivanytskyi, *Bosonic dark matter in neutron stars and its effect on gravitational wave signal*, *Phys. Rev. D* **105** (2022) 023001 [[2109.03801](#)].
- [27] E. Giangrandi, V. Sagun, O. Ivanytskyi, C. Providência and T. Dietrich, *The Effects of Self-interacting Bosonic Dark Matter on Neutron Star Properties*, *Astrophys. J.* **953** (2023) 115 [[2209.10905](#)].
- [28] S. Shakeri and D.R. Karkevandi, *Bosonic dark matter in light of the NICER precise mass-radius measurements*, *Phys. Rev. D* **109** (2024) 043029 [[2210.17308](#)].
- [29] C.H. Lenzi, M. Dutra, O. Lourenço, L.L. Lopes and D.P. Menezes, *Dark matter effects on hybrid star properties*, *Eur. Phys. J. C* **83** (2023) 266 [[2212.12615](#)].
- [30] S. Pal, S. Podder, D. Sen and G. Chaudhuri, *Speed of sound in hybrid stars and the role of bag pressure in the emergence of special points on the M-R variation of hybrid stars*, *Phys. Rev. D* **107** (2023) 063019 [[2303.04653](#)].
- [31] N. Glendenning, *Compact Stars: Nuclear Physics, Particle Physics and General Relativity*, Astronomy and Astrophysics Library, Springer New York (2012).
- [32] A. Chodos, R.L. Jaffe, K. Johnson, C.B. Thorn and V.F. Weisskopf, *New extended model of hadrons*, *Phys. Rev. D* **9** (1974) 3471.

- [33] G. Panotopoulos and I. Lopes, *Dark matter effect on realistic equation of state in neutron stars*, *Phys. Rev. D* **96** (2017) 083004 [[1709.06312](#)].
- [34] S.A. Bhat and A. Paul, *Cooling of Dark-Matter Admixed Neutron Stars with density-dependent Equation of State*, *Eur. Phys. J. C* **80** (2020) 544 [[1905.12483](#)].
- [35] A. Das, T. Malik and A.C. Nayak, *Confronting nuclear equation of state in the presence of dark matter using GW170817 observation in relativistic mean field theory approach*, *Phys. Rev. D* **99** (2019) 043016 [[1807.10013](#)].
- [36] M. Dutra, C.H. Lenzi and O. Lourenço, *Dark particle mass effects on neutron star properties from a short-range correlated hadronic model*, *Mon. Not. Roy. Astron. Soc.* **517** (2022) 4265 [[2211.10263](#)].
- [37] O. Lourenço, C.H. Lenzi, T. Frederico and M. Dutra, *Dark matter effects on tidal deformabilities and moment of inertia in a hadronic model with short-range correlations*, *Phys. Rev. D* **106** (2022) 043010.
- [38] H.C. Das, A. Kumar and S.K. Patra, *Dark matter admixed neutron star as a possible compact component in the GW190814 merger event*, *Phys. Rev. D* **104** (2021) 063028 [[2109.01853](#)].
- [39] A. Guha and D. Sen, *Feeble DM-SM interaction via new scalar and vector mediators in rotating neutron stars*, *JCAP* **09** (2021) 027 [[2106.10353](#)].
- [40] D. Sen and A. Guha, *Vector dark boson mediated feeble interaction between fermionic dark matter and strange quark matter in quark stars*, *Mon. Not. Roy. Astron. Soc.* **517** (2022) 518 [[2209.09021](#)].
- [41] L. Tolos, J. Schaffner-Bielich and Y. Dengler, *Dark Compact Planets*, *Phys. Rev. D* **92** (2015) 123002 [[1507.08197](#)].
- [42] A. Guha and D. Sen, *Constraining the mass of fermionic dark matter from its feeble interaction with hadronic matter via dark mediators in neutron stars*, *Phys. Rev. D* **109** (2024) 043038 [[2401.14419](#)].
- [43] G.A. Lalazissis, J. König and P. Ring, *A New parametrization for the Lagrangian density of relativistic mean field theory*, *Phys. Rev. C* **55** (1997) 540 [[nucl-th/9607039](#)].
- [44] F.J. Fattoyev, C.J. Horowitz, J. Piekarewicz and G. Shen, *Relativistic effective interaction for nuclei, giant resonances, and neutron stars*, *Phys. Rev. C* **82** (2010) 055803 [[1008.3030](#)].
- [45] W.-C. Chen and J. Piekarewicz, *Building relativistic mean field models for finite nuclei and neutron stars*, *Phys. Rev. C* **90** (2014) 044305 [[1408.4159](#)].